A Compliance-centric View of Grasping

Clemens EPPNER Georg BARTELS Oliver BROCK

TECHNICAL REPORT

№ RBO-2012-01

of the Robotics and Biology Laboratory,
Department of Computer Engineering and Microelectronics,
Technische Universität Berlin

February 2012

A Compliance-centric View of Grasping

Clemens Eppner Georg Bartels Oliver Brock

Abstract

We advocate the central importance of compliance for grasp performance and demonstrate that grasp algorithms can achieve robust performance by explicitly considering and exploiting mechanical compliance of the grasping hand. Specifically, we consider the problem of robust grasping in the absence of a priori object models, focusing on object capture and grasp stability under variations of object shape for a given robotic hand. We present a simple characterization of the relationship between hand compliance, object shape, and grasp success. Based on this hypothesis, we devise a compliance-centric grasping algorithm. Real-world experiments show that this algorithm outperforms compliance-agnostic grasping, eliminates the need for explicit contact state planning, and simplifies the perceptual requirements when no a priori information about the environment is available.

1 Introduction

Compliance plays a critical role in any real-world grasping experiment. Compliance describes the ability of the grasper and the object to match each other's shape in response to contact forces without explicit sensing and control. Compliance is omnipresent in robotic grasping experiments, be it intentional or not. We believe that it is a major contributor to the experimental success of existing grasping approaches.

We emphasize the centrality of compliance for grasping with several examples from machine and human grasping. When robotic hands are designed to be highly compliant, they achieve good grasping performance without the need for complex grasp planning or control. The SDM hand, for example, realizes astonishing grasping performance by mechanically balancing contact forces among its four flexible fingers [10]. A different grasping mechanism, based on highly compliant granular material inside an elastic bag, conforms to object shapes effortlessly, thereby achieving remarkable grasping versatility and robustness [2].

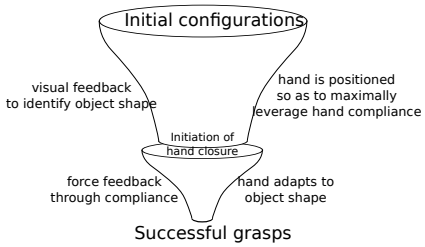

Figure 1: We visualize grasping algorithms as two consecutive funnels, transforming initial configurations into successful grasps through the use of feedback. The first funnel leverages visual feedback to transform the starting conformation into a configuration that lies inside the entrance of the second funnel. The second funnel relies on the force interaction between the hand and the object and the hand's compliance to obtain a successful grasp. In this paper, we introduce a visual method to realize the first funnel and show that it leads to configurations in the entrance of the second funnel and hence to robust grasping without prior object models.

Compliance of the object to be grasped is also advantageous to grasping. This is obvious for flexible objects. But even rigid objects exhibit compliance when they can adjust their position relative to the hand. In the context of bin-picking, simple grippers can take advantage of object motion to achieve robust grasping [15]. And the push-grasping approach relies on this compliance to improve grasping in the presence of sensing uncertainty and clutter [9].

Humans extensively rely on compliance to achieve robust grasping. Experiments performed by Santello et al. [24] showed that humans use a small set of pre-grasp hand postures when grasping objects of widely varying shapes. Robust grasping then seems to be the result of "simply closing the hand", leveraging the compliance of the skeletal hand structure, muscles, tendons, and skin to achieve complementarity of hand and object geometry.

In spite of the striking effect compliance has on grasping performance in the real world, most existing grasp planners do not deliberately leverage compliance to improve performance. In this paper, we will explore how this can be changed.

Our goal is to leverage hand compliance in the development of novel grasping algorithms. The underlying hypothesis is as follows: compliance in the hand, irrespective of whether it is achieved passively or actively, can be viewed as a funnel that transforms configurations in a large region of the configuration space into a configuration in the smaller region of successful grasps (see Figure 1, the bottom part of the funnel captures the compliance of the hand). Compliance therefore introduces robustness to uncertainty and reduces sensing requirements.

Given this hypothesis, a compliance-centric grasping algorithm must a) characterize the entrance to the bottom part of the funnel and b) transfer initial configuration into those that lie at its entrance. This is illustrated by the top part

(a) $P_{\text{success}} > 0.9$ **(b)** $P_{\text{success}} > 0.6$ **(c)** $P_{\text{success}} > 0.3$

Figure 2: *Cartoons illustrating the effect of complementarity of compliance mode and object shape on grasping success:* Each of the three cartoons (a)–(c) represents a cut parallel to the x/y-plane through a three-dimensional shape (see text). The polar coordinates (r, θ) correspond to object size and object shape. The yellow, red, and green regions indicate the parts of the plane where grasping success exceeds a given threshold. The red *annulus* corresponds to a region of the space in which caging effects dominate the probability of grasp success. The radially emanating rays of the yellow *sun* correspond to a particular compliance mode of the hand. If the shape of the object matches the compliance mode, grasp success in increased radially. As object size increases, the entrance of the funnel of hand poses narrows as fewer poses yield successful grasps. The inverted, green *flower* around the origin characterizes a region in which precision grasps possibly require different hand compliances than the ones considered in this paper.

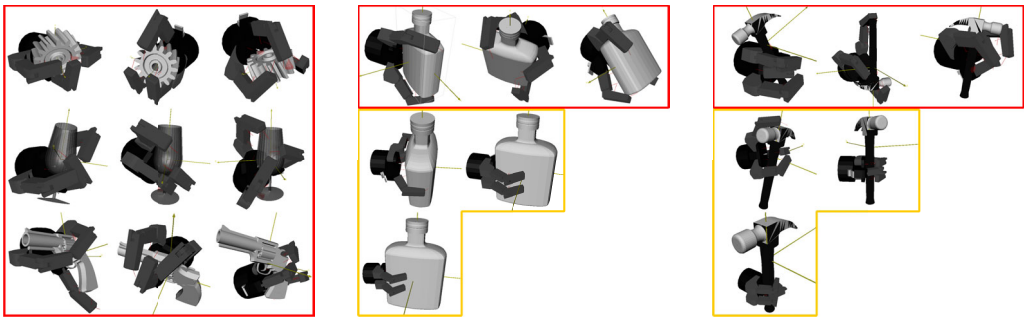

(a) Annulus **(b)** Sun ray: box **(c)** Sun ray: cylinder

Figure 3: *Example grasps for different regions of the SFA cartoon, frame colors indicate SFA regions:* Panel (d) for three objects (rows) within the annulus, each object corresponding to a different angle of the polar coordinate system. For objects in the annulus, grasp success is strongly influenced by caging effects and less by shape complementarity. As object size increases, the influence of shape complementarity and therefore compliance mode and hand pose on grasp success increases, as illustrated for two objects with distinct shapes in panels (e) and (f). In these panels, the first row corresponds to object sizes in the annulus. In each successive row, object size increases; fewer hand poses will lead to successful grasps and the width of the entrance to the funnel (and the sun ray) decreases.

of the funnel in Figure 1. We will show that compliance-centric grasping algorithms exhibit robust grasping performance, significantly reduce the requirements on perception, and eliminate the need for explicit planning of contact points.

In the remainder of this paper, we first propose a characterization of the effect of hand compliance on grasp success in Section 2. We then validate this characterization by showing its predictiveness of grasp success in simulation experiments (Section 3). In Section 4 we use insights derived from our characterization to develop a specific compliance-centric grasp algorithm; perception will turn out to be a central component to identify the entrance of the bottom funnel induced by hand compliance. We evaluate our approach to perception in real-world experiments in Section 5. These experiments will show that the output of our visual primitives correlates with grasp success, which implies that they are able to identify the entrance to the funnel induced by hand compliance. We then show in Section 6 that compliance-centric grasping outperforms compliance-agnostic planning in real-world grasping experiments, even when we grant the latter access to a priori world models. We defer the discussion of related work to the end of the paper so that we can better highlight the differences between compliance-centric and compliance-agnostic grasp algorithms.

2 Characterizing the effect of hand compliance on grasp success

In this paper, *compliance* refers to the hand's ability to use feedback to adapt its shape to that of the grasped object. This can happen explicitly through tactile sensors and controllers, for example, or implicitly through underactuation or mechanical compliance in the hand's components. The *compliance mode* of a hand is given by a specification of the intrinsic degrees of freedom of the hand and a controller that closes the fingers compliantly. A *compliance-centric grasp* is specified by a hand pose and a compliance mode. Successful compliance-centric grasps lie in the entrance of the bottom funnel in Figure 1. A *grasp strategy* is an algorithm for selecting compliance-centric grasps from sensor data in the absence of a priori geometric models (the top funnel in Figure 1.

In this section, we derive a cartoon-like characterization of the effect of shape complementarity between the hand's compliance mode and object shape on grasp success. This will enable us to characterize the entrance to the bottom funnel in Figure 1. In the subsequent section, we will validate this characterization experimentally.

We consider the problem of robust grasping with hands in the absence of a priori object models. We focus on aspects of object capture and grasp stability under

variations of object shape for a given robotic hand. In our discussion of grasping compliance, we will not consider clutter, placing objects, task constraints, or in-hand manipulation [16]; this can be the subject of subsequent studies of compliance-centric grasping algorithms.

Robotic hands may be configured to exhibit different modes of compliance. A compliance mode specifies a pre-grasp shape (e.g. cylindrical, spherical, etc.) of the hand and a controller to compliantly close the fingers. A compliance mode thus captures the hand's ability to conform to a particular object geometry in the absence of explicit sensing and control. We must identify the compliance mode of the hand that maximizes the likelihood of reaching shape complementarity with the object. We assume that shape complementarity then leads to object capture and grasp stability.[1]

We must find, for a given object and a given hand, the compliance funnel with the largest opening. The shape of the funnel depends on the likelihood of reaching shape complementarity through compliance. We therefore must understand the different effects of achieving shape complementarity as a function of compliance mode.

Our characterization of the effect of shape complementarity between hand and object on grasp success is illustrated in a cartoon-like fashion in Figures 2a to 2c. The three panels each show a cut through a three dimensional shape;[2] The cuts consist of three regions, shaped like a sun, an annulus, and an inverted flower; we therefore refer to our characterization as *SFA*. A description of SFA is contained in the caption of Figure 3.

In this paper, we focus on grasping on objects in the annulus and the sun of the SFA. We will leave for future work the presumable more complex compliance strategies required for robust grasping in the flower, where precision grasps live.[3]

[1]We deliberately disregard the notions of form and force closure in favor of the vague notion of shape complementarity, as the former are only meaningful in the presence of adequate geometric models of hand and object, and given an accurate characterization of contact dynamics; these assumptions are too strict for general grasping in unstructured environments.

[2]This shape is not important for understanding the paper. It can be imagined as the volume under a surface obtained by plotting for each point in the shape/size space of Figure (a) the highest achievable success rate of an "oracle-provided" optimal grasping strategy.

[3]An informal survey of the literature in robotic grasping imparts the impression that many of the reported grasping experiments lie in the annulus of the SFA where grasping strategies are less discriminative. This observation should impact future grasping benchmarks. One could argue that experiments in the annulus are appropriate as most objects in the real world lie in the annulus by design. Others may want to counter that general grasping can only be benchmarked outside the annulus.

3 Validation of compliance characterization

In this section we describe simulation experiments to provide quantitative support for the SFA characterization. We focus on validating our characterization of the annulus and of the grasp success variations along the rays of the sun. Later, in Section 5, we will provide additional real-world experimental evidence to support our view that the rays of the sun represent separate, shape-specific regions of high grasp success and that the annulus is relatively insensitive to the hand's compliance mode.

3.1 Experimental setup

For all experiments in this paper—simulation and real-world—we use the BarrettHand, a three-fingered 4-DoF hand. We employ to different compliance modes, spherical (adjustable spread between fingers 1 and 2 set to 120°) and cylindrical (spread set to 0°). The corresponding grasp controller invokes the torque close mode on the three fingers. Compliance is achieved with a breakaway mechanism, allowing the distal link of each finger to continue to close on an object when proximal link is already in contact with it. A distal contact stops the motion of both links.[4]

We simulate a large number of quasi-static grasps using OpenRAVE [8]. For each grasp we calculate the commonly used ε-grasp quality metric [12], which indicates the minimum magnitude force required to break the grasp. Grasping experiments were conducted with spheres, cubes, and cylinders. The results for sphere and cylinder match closely and we will discuss results for cylinder.

Object shapes are deliberately kept simple to make a near-optimal grasping strategy obvious. Such a strategy is required to draw meaningful conclusions about the SFA, as it captures intuition about optimal strategies. For spheres, the robot employs the spherical compliance mode, approaches the center of the sphere with the center of the palm until contact is made, and then closes the fingers. For cubes (and cylinders), the robot employs the cylindrical compliance mode; during the approach the hand is aligned to the major axes of the object.

3.2 Results and discussion

The top graph in each of the four panels in Figure 4 show grasp quality as a function of object size and hand pose error along either the x of y direction. The graph below the color plot shows as a function of object size the mean grasp

[4]There is debate in the literature on whether the breakaway mechanism can be considered compliant. According to our definition it constitutes passive compliance, as it permits the hand to achieve shape complementarity in response to contact forces.

quality $\varepsilon_{\text{mean}}$ (red solid line) and the maximum grasp quality ε_{max} (green dotted line) across all pose errors. The blue dashed line shows the grasp quality ε_0 in the absence of a pose error. For the cylindrical grasp experiments with cubes, the fingers close along the y-axis.

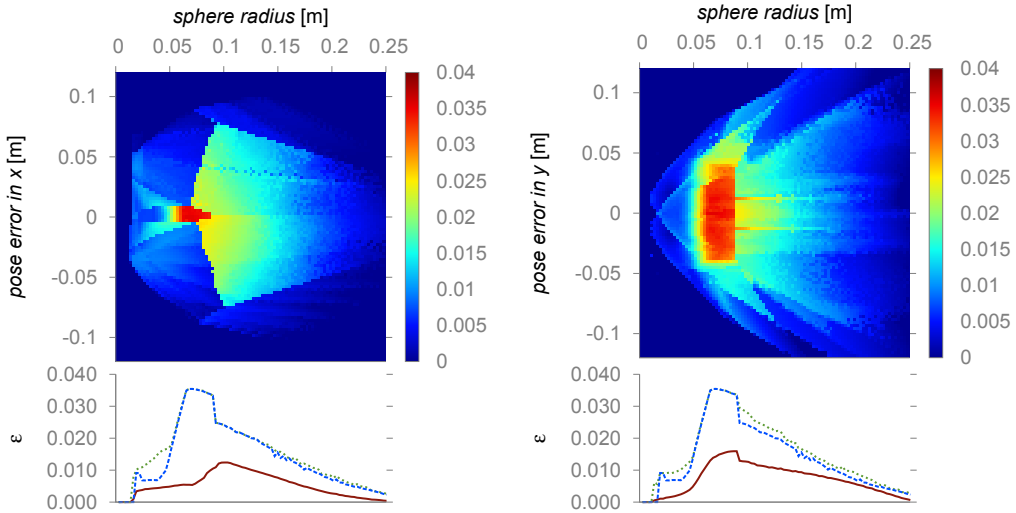

(a) Sphere: pose error in x

(b) Sphere: pose error in y

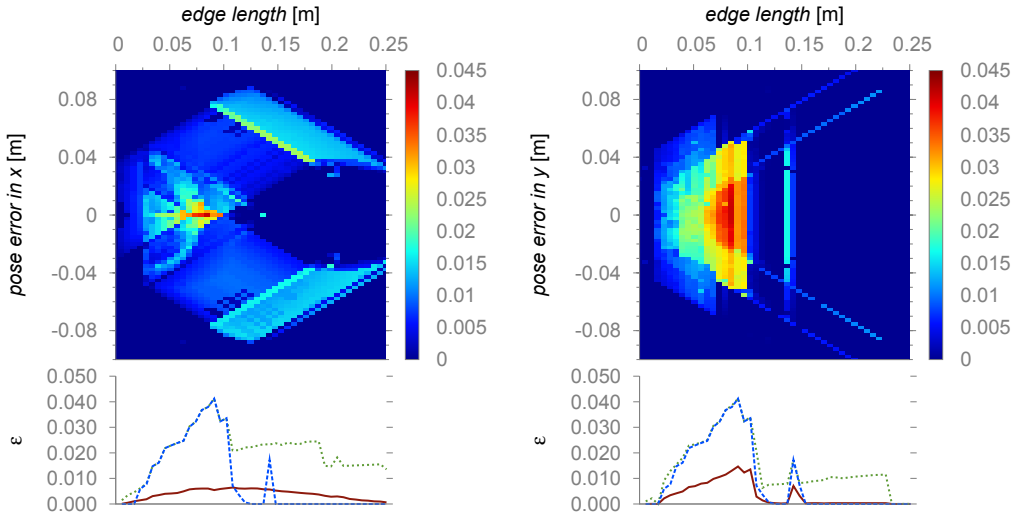

(c) Cube: pose error in x

(d) Cube: pose error in y

Figure 4: Grasp quality as a function of object size and pose error; the color scale indicates the grasp quality measure ε; in the plots the red solid line corresponds to $\varepsilon_{\text{mean}}$, the green dotted line shows ε_{max}, and the blue dashed line ε_0

The close match between ε_{max} and ε_0 in all graphs provides a sanity check for

the chosen grasp strategies. The color plots together with the curves for $\varepsilon_{\max}$ and ε_{avg} provide an low-dimensional estimate of the width of the funnel.

All graphs show peak grasp qualities for medium object size, providing evidence for the annulus. In the annulus, grasp quality is high and the funnel is wide. Experiments in Section 5 will also show that grasp quality inside the annulus is less coupled to the compliance mode of the hand.

The data also shows that grasp quality, indicative of the probability of grasp success, decreases as object size increases beyond the annulus. The sudden drop in grasp quality in Figure 4d is the result of only two fingers making contact with the cube. Inside the flower, grasp quality is poor, indicating that different compliance modes might be required for robust grasping.

4 Detecting shape resemblance for compliance-centric grasping

To fully take advantage of hand compliance in grasping, we must find the compliance mode of the hand that best matches the object shape. This will give us the widest bottom funnel in Figure 1. Doing so does not require an exact representation of the object's shape. Instead, we must obtain some estimate of how well the hand can accommodate object's shape in a particular compliance mode—we call this *shape resemblance*. In addition to the shape resemblance, which indicates the appropriate compliance mode, we must extract sufficient information to determine a hand pose centered in the compliance funnel. We believe that the identification of compliance mode and hand pose are much simpler perception problems than the one required for compliance-agnostic planning, namely, the acquisition of an accurate three-dimensional geometric models. Furthermore, the need for the planning of contact states is completely eliminated.

O'Regan and Noë [22] state in human visual experience "that the visual quality of shape *is precisely* the set of all potential distortions that the shape undergoes when it is moved relative to us, or when we move relative to it." They refer to these sets as *sensorimotor contingencies*. This active vision-based characterization of shape seems well suited for our purposes. We observe the changes of object silhouettes under object motion and represent different object shapes by different qualitative changes. How this can be done will be described in this section. Our hope, confirmed in the experimental evaluation in the next section, is that the resulting visual primitives will be robust and yield good entrances to folding funnels, as they only capture the overall shape of the object, naturally and effortlessly ignoring unimportant details.

In the remainder of this section we will describe five visual primitives based

on active vision sensorimotor contingencies. Three of these visual primitives determine shape resemblance for a specific shape: *sphere, box, and cylinder*. In addition to shape resemblance, the visual primitives must acquire additional information required for the execution of a compliant grasp: position, orientation, and size of the object. This information is sufficient to execute the appropriate compliant grasp.

The simplicity and effectiveness of all active visual primitives is based on the concept of active vision: the motion of the camera is controlled so as to maximize the visual information obtained from the image stream. The advantage of active vision over dynamic vision (just knowing how the camera moves) when estimating the parameters of simple geometric objects was shown by Chaumette et al. [4]. Our visual primitives are similar in spirit to the ones presented there.

The basic idea underlying the visual shape primitives is as follows: When a camera moves on an imagined sphere around the object of interest while pointing the optical axis pointed towards the center of the object (sphere), the changes in the silhouette of the object reveal information about the object's shape. One might call this the sensorimotor contingencies of the object [22]. We take advantage of this effect to discriminate between shapes.

To control the camera motion so as to remain on this imagined sphere around an object, we need to estimate spatial information. This is accomplished by the depth primitive and the principal axis primitive.

Depth primitive As we are using an eye-in-hand setting with a monocular camera, we're lacking instantaneous depth information. To retrieve depth, we designed an active vision controller that converges to a concentric trajectory around the object's center (an arc on the imagined sphere). The controller moves the camera so as to keep the center of the object's projection in the center of the image. In each time step, the controller commands the camera according to its current depth estimate. Motion of the object's center in the image leads to a correction of the depth estimate. When the controller convergence, the camera moves on a sphere around the object center. The sphere's radius is equal to the estimated depth.

Principal axis primitive Similar to the estimation of depth we actively estimate the main axis of an object. We derive the principal axis of the detected blob in the image plane via its second order central moments. A visual servoing loop keeps this axes aligned w.r.t. the image border. We are using the expected invariance of the axis' orientation during camera motion to update an estimate of the axis orientation in space. The camera motion describes again an arc around the object's principal axis. This motion results in optimal information gain for the estimation of lines in space [4].

The visual primitives for estimating depth and the principal axis are executed in parallel, as their desired exploratory motions lie in the nullspace of each other. After their convergence, we invoke the shape resemblance primitives, all of which execute in parallel.

Shape resemblance primitives To assess the shape resemblance of the object to the shapes of a box, a sphere, and a cylinder, we determine two simple visual properties of the object's silhouette: its contour area and eccentricity. The resemblance with a particular shape class depends only on the variance of these two properties during the camera motion around the object. A constant projected size and an eccentricity close to 1 indicate a sphere-like object. A constant contour area but an eccentricity $\gg 1$ suggest an object that is rotationally symmetric along its principal axis. We refer to this as the cylindrical shape resemblance primitive. A box shape resemblance is detected when the eccentricity $\gg 1$ and the projected size varies throughout the camera's motion around the object.

Our experiments will show that the resulting shape information is sufficient for robust grasping of unmodeled objects. Of course, it is not practical to move the camera around an object prior to each grasp, as is necessary in this first version of our grasp algorithm. However, we view this algorithm as a proof of concept. In the future, the need for active camera motion can be significantly reduced in most cases by first deriving a shape hypothesis from 2D vision and then confirming this hypothesis through minimal camera motion. If the 2D hypothesis cannot be confirmed, the robot uses the procedure above to recover.

5 Validation of relationship between shape resemblance and grasp success

Our compliance-centric grasping algorithm rests on the assumption that the shape resemblance values determined by visual strategies are indicative of width of the entrance to the bottom funnel in Figure 1. The width of the funnel should lead to robustness in the grasping process. Hence, shape resemblance values should correspond to grasp success for the corresponding compliance-based grasp. We will now test this assumption in real-world experiments.

5.1 Experimental setup

For our real-world grasping experiments, we use a 7-DoF Barrett WAM in combination with a BarrettHand and a PointGrey Firefly camera mounted on the wrist. Fig. 5 shows the objects we used: a banana, apple, pepper, sponge, spectacle

case, toy bridge, soccer ball, game box, and a cylindrical bottle case. Given our knowledge of the hand's grasping volume, the first six objects were chosen to lie in the annulus. The size of the remaining three objects (soccer ball, game box, bottle case) places them outside of the annulus. Each represents a different class of object shapes, thus representing a different ray of the sun. To simplify the segmentation problem for the visual primitives, the game box and bottle case were wrapped in yellow paper.

We employed three compliant grasps: spherical grasp, cylindrical grasp, and box grasp, each corresponding to one of the visual strategies described in Section 4. The cylindrical grasp and the box grasp both share the cylindrical compliance mode of the hand but differ in the way they select the appropriate hand pose and approach direction.

Our experimental procedure is as follows: One object at a time is placed inside the robot's workspace on a white table in a specified pose. In each grasping trial, the visual primitives is used to determine the shape resemblance. Subsequently, the corresponding compliant grasp is executed. For each of the nine objects and three compliant grasps we conducted 10 trials, for a total of 270 grasping trials. A grasp was deemed successful if after lifting the object $10cm$ off the table no obvious slippage occurred within $10s$.

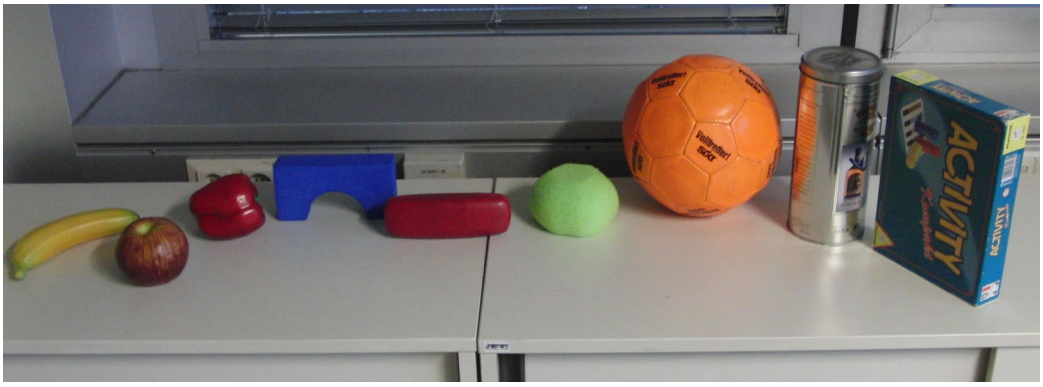

Figure 5: Objects used in the experiments

5.2 Results and Discussion

The outcome of this experiment is shown as a scatter plot in Fig. 6. The color of the circles represents the visual primitive/compliant grasp (box is red, spherical is green, cylindrical is blue). Each circle's size represents the grasp success rate. The circle center's y-coordinates indicates the shape resemblance value determined by the corresponding visual strategy. The circle with the highest y-coordinate for

each object represents the compliant grasp selected by our grasp algorithm; its diameter therefore represents the algorithm's success rate for that object. The averaged success rate over all objects is 95.6% (86 out of 90 trials, two failures with the soccer ball, one with the spectacle case and the bell pepper).

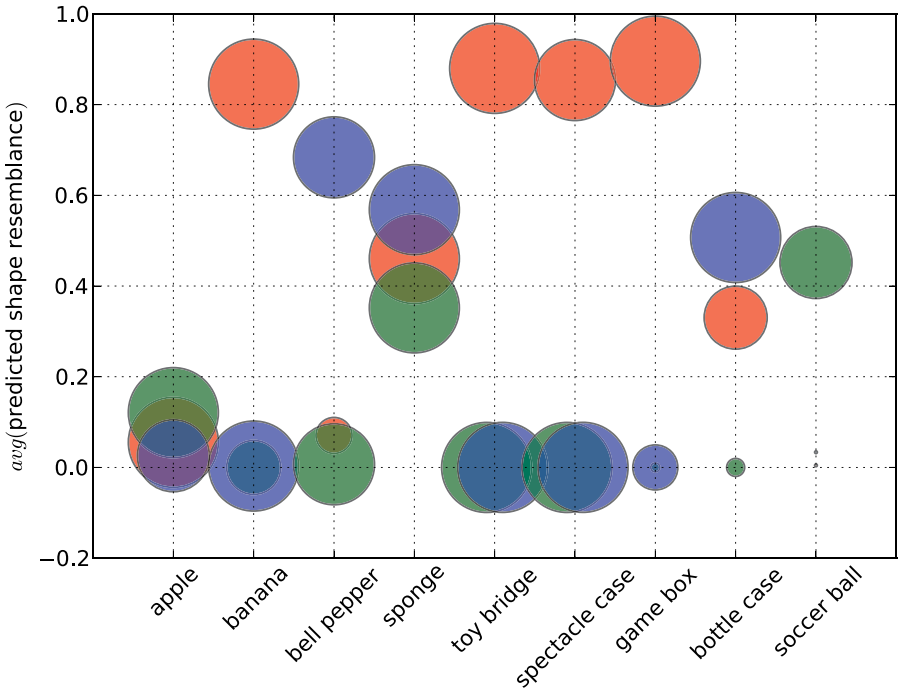

Figure 6: Shape resemblance determined by the visual primitives: box (red spheres), spherical (green), and cylindrical (blue); the diameter of the spheres indicates the success of the corresponding compliant grasp

The results show that inside the annulus (six objects to the left) the three grasping strategies not not differ significantly in their grasp success. The minor variations in the case of apple, banana, and bell pepper are correctly detected by the visual strategies: they select the compliant grasp with the highest success rate. This indicates that even in the annulus there is a good match between shape resemblance value and predicted grasp success of the corresponding compliant grasp. For the spectacle case, however, we select the weakest strategy, even though it fails only once out of ten trials and we still achieve a success rate of 90%.

As expected, grasp success varies widely in the rays of the sun. The visual resemblance detected by the visual primitives strongly correlates with grasping success of the corresponding compliant grasp. For each of the objects, a different

compliant grasp is most appropriate, showing that the rays of the sun are separate, shape- and compliant grasp-specific regions of high grasp success probability. In the case of the soccer ball, only the spherical compliant grasp is successful at all.

These results provide further support for the SFA characterization. They show that visual resemblance is a good measure for selecting compliant grasps and a good predictor of grasp success. The results also show that our spherical visual primitive is too selective, as it results in a visual resemblance value of less than 0.5 for a perfect sphere.

6 Comparison of compliance-centric and compliance-agnostic grasping

In our final set of experiments, we compare the proposed compliance-centric grasp algorithm to a specific compliance-agnostic grasp planner. We show that our algorithm outperforms the compliance-agnostic planner, even after we provide the latter with accurate a priori object models, something that could be considered an important advantage over our method.

6.1 Experimental setup

For the experimental comparison we chose the Eigengrasp planner [6], implemented inside the GraspIt! framework [17]. Our reason for choosing this planner were its relative recency, its popularity in terms of citations, and the availability of the source code.

We took great care in determining geometric models of six of the objects in Figure 5 (all except the fruits and vegetable), performing several independent measurements for each. We included object-specific, conservative estimates of surface friction in the models.

To generate candidate grasps with the Eigengrasp planner, we used 70,000 iterations of simulated annealing, setting the energy formulation as "hand+object". We eliminated candidate grasps for which no inverse kinematic solution for the arm existed (this only happened for two of the six objects objects and did not affect the two highest-quality grasps). We then selected the three best grasps, performing ten trials for each, for a total of 180 grasp attempts. The exact pose of the object was an input to the grasp attempt. Grasp success was measured as before.

For comparison, we calculated two measures of success for the Eigengrasp planner. The *average* success rate includes all 30 grasps per object, while the *best* success rate only represents the most successful of the three planned grasps. Note that the second metric selects the best grasp in hindsight, after all experiments are

performed.

6.2 Results and discussion

Figure 7 compares the grasp success obtained with the Eigengrasp planner to our compliance-centric algorithm. Among the objects inside the annulus, only the spectacle case shows significant difference in grasp success. Our algorithm outperforms the Eigengrasp planner in either metric. In the rays of the sun (bottle case and soccer ball), the Eigengrasp planner fails in all grasp attempts. This could be an indication that the advantage of compliance-centric grasping increase as we reach the boundary of the SFA. In the case of the box, however, both grasp methods achieve 100% success.

Overall, our compliance-centric grasp algorithm always performs better or as good as the Eigengrasp planner, providing real-world experimental support for the funnel-based view of compliance-centric grasping in Figure 1. The grasp results demonstrate that the proposed visual primitives successfully identify configurations in the entrance to the bottom part of the funnel. These visual primitives are simple and effective. They eliminate the need for explicit contact planning, supporting the claim that hand compliance should become a central consideration in robot grasping.

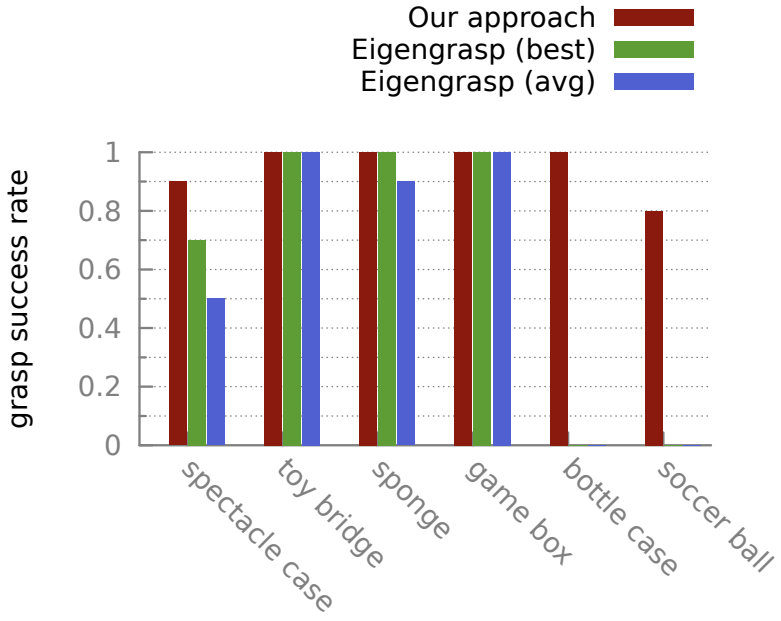

Figure 7: Comparison of compliance-centric grasp algorithm with Eigengrasp planner

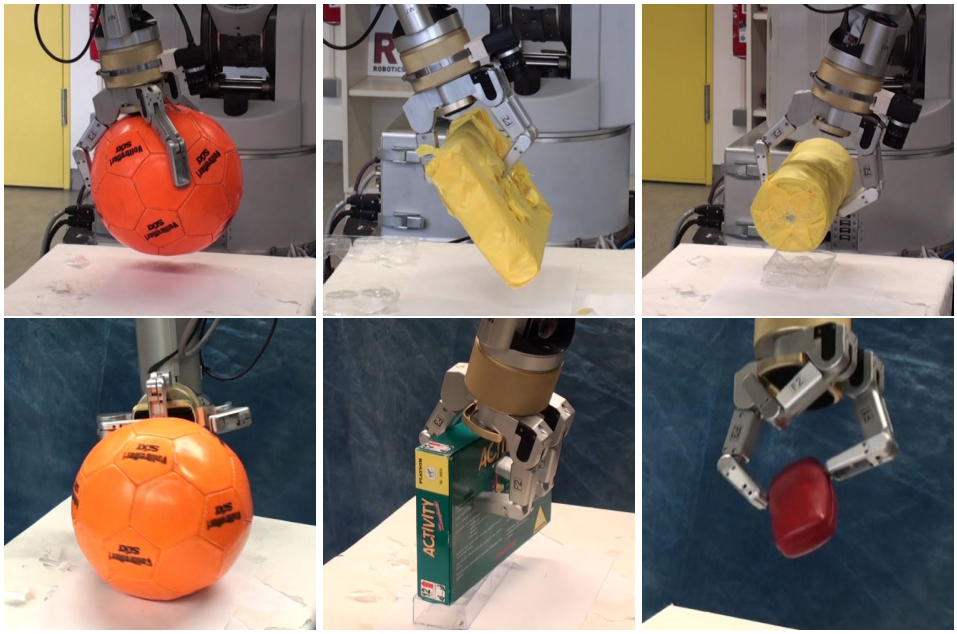

Figure 8: Top: grasps of the compliance-centric algorithm; **Bottom:** – grasps of the Eigengrasp planner

7 Related Work

In this section we will discuss related grasping approaches. We focus on work that leverage hand compliance and work that is based on little or no a-priori object knowledge.

7.1 Approaches that leverage knowledge about compliance

Ciocarlie and Allen [6] synthesize grasps based on the idea that the intrinsic DOF of a hand can be mapped into a lower dimensional sub-space, without losing much expressiveness. This way they can search the space of possible pre-grasps much faster. In executing grasps, they implicitly rely on compliance when closing the fingers. We compared our algorithm with this approach.

Miller et al. [18] present a planner that uses heuristics which describe how to grasp basic shapes, such as boxes, cones, spheres and cylinders. Their pre-grasps and approach strategies resemble our compliant grasp strategies. However, they rely on a known decomposition of the object, ignoring this non-trivial perception problem. The planner also does not explicitly account for compliance.

Huebner and Kragic [14] use an object representation based on box primitives to select grasps. This implicitly relies on compliance during grasping to compensate for the approximation error introduced by the primitives.

The grasp approach presented in Dune et al. [11] also relies on active vision to acquire information about object shape but then relies on shape approximation with quadrics to represent this information. Again, by relying on a shape approximation, the approach implicitly depends on hand compliance.

Diankov et al. [7] presents a planner that grasps handles to manipulate kinematic structures such as doors. This approach replaces the force closure criterion for grasps with a caging constraint. The execution of caged grasps will also benefit from compliance.

Diankov [8] proposes to select robust grasps by perturbing the planned approach direction and wrist angle during grasp planning. This can be interpreted as determining the width of the entrance of the compliance funnel for a grasp through many repeated grasp simulations based on a world model. We show that it is easier to extract this information from sensor data and to consider compliance explicitly.

7.2 Approaches that use a-priori knowledge and perception

Many grasping algorithms approach the problem from a purely geometric perspective. These approaches introduce grasp quality metrics and use them to synthesize grasps in 2D or 3D [20, 21, 5, 12]. They all assume that complete object knowledge is accessible up to an arbitrary degree. Interestingly enough, Balasubramanian et al. [1] showed that a much simpler quality measure, which was used by humans when controlling robotic hardware, produces more reliable grasps. These findings match our conclusions regarding the relationship between compliance and grasp performance closely. The presented compliant grasping strategies also maximize orthogonality with respect to the objects principal axes.

Other approaches separate the grasping problem into two stages: building object models and planning on top of these representations. Apart from the ones above, which use shape approximations, a variety of vision-based approaches exist. Hauck et al. [13] use a stereo-vision system to detect and triangulate grasping points on the silhouette of an object. Morales et al. [19] assume planar extruded objects, for which they plan two- and three-fingered grasps based on the object's detected contour. In [25] a classifier for detecting grasping points in images is learned from a set of labeled training examples. The resulting classifier usually prefers pairs of edge-like features, ignoring any depth information.

A third group of grasping approaches updates grasp hypotheses continuously by integrating sensor measurements. Calli et al. [3] use an eye-in-hand system and apply a visual servoing scheme that maximizes the curvature of the object silhouette, thus leading the hand to concave parts of the object. Platt et al. [23] use tactile feedback to refine a grasp after initial contact by controlling two opposing

fingers along the object surface. They show that their strategy converges to force-closure for arbitrary convex objects.

8 Conclusion

The explicit consideration of hand compliance in robotic grasping improves performance and robustness. We argued that grasp algorithms should be compliance-centric, i.e. they should deliberately take advantage of hand compliance to improve performance. In this paper, we presented a first exploration into this direction. We provided a cartoon-ish characterization of the influence of shape complementarity between a hand's compliance mode and the object's shape. Through experimental validation we showed that this characterization captures some interesting aspects of compliant grasping. The resulting insights lead to the development of a set of active vision-based grasp strategies for different compliant modes. These compliance-centric strategies exhibit robust real-world performance, outperforming a compliance-agnostic grasping strategy. At the same time, by letting the compliance of the hardware "sort out the details" of the best hand configuration for a robust grasp, our approach eliminates the need for planning specific point contacts and thus the necessity for detailed geometric models of the hand and object. Instead, we employ simple visual strategies based on sensorimotor contingencies to identify appropriate compliant grasps. Giving compliance a central role in grasping leads to simple algorithms with robust performance.

Acknowledgments

We gratefully acknowledge the funding provided by the Alexander von Humboldt foundation and the Federal Ministry of Education and Research (BMBF) and through the First-MM project (European Commission, FP7-ICT-248258). We thank SimLab for their support. Finally, we thank Erik Learned-Miller for insightful discussions.

References

[1] R. Balasubramanian, Ling Xu, P. D Brook, J. R Smith, and Y. Matsuoka. Human-guided grasp measures improve grasp robustness on physical robot. In *2010 IEEE Intl. Conf. on Robotics and Automation (ICRA)*, pages 2294–2301, 2010.

[2] E. Brown, N. Rodenberg, J. Amend, A. Mozeika, E. Steltz, M. R. Zakin, H. Lipson, and H. M. Jaeger. Universal robotic gripper based on the jamming of granular material. *Proc. of the National Academy of Sciences*, 107(44):18809–18814, 2010.

[3] B. Calli, M. Wisse, and P. Jonker. Grasping of unknown objects via curvature maximization using active vision. In *2011 IEEE/RSJ Intl. Conf. on Int. Robots and Systems (IROS)*, 2011.

[4] F. Chaumette, S. Boukir, P. Bouthemy, and D. Juvin. Structure from controlled motion. *IEEE Transactions on Pattern Analysis and Machine Intelligence*, 18(5): 492–504, 1996.

[5] I-Ming Chen and J. W Burdick. Finding antipodal point grasps on irregularly shaped objects. *IEEE Transactions on Robotics and Automation*, 9(4):507–512, 1993.

[6] Matei T. Ciocarlie and Peter K. Allen. Hand posture subspaces for dexterous robotic grasping. *The Intl. Journal of Robotics Research*, 28(7):851 –867, 2009.

[7] R. Diankov, S. S Srinivasa, D. Ferguson, and J. Kuffner. Manipulation planning with caging grasps. In *8th IEEE-RAS Intl. Conf. on Humanoid Robots, 2008. Humanoids 2008*, pages 285–292, 2008.

[8] Rosen Diankov. *Automated Construction of Robotic Manipulation Programs*. PhD thesis, Carnegie Mellon University, Robotics Institute, 2010.

[9] M.R. Dogar and S.S. Srinivasa. Push-grasping with dexterous hands: Mechanics and a method. In *2010 IEEE/RSJ Intl. Conf. on Intelligent Robots and Systems (IROS)*, page 21232130, 2010.

[10] Aaron M. Dollar and Robert D. Howe. The highly adaptive SDM hand: Design and performance evaluation. *The Intl. Journal of Robotics Research*, 29(5):585 –597, 2010.

[11] C. Dune, E. Marchand, C. Collowet, and C. Leroux. Active rough shape estimation of unknown objects. In *IEEE/RSJ Intl. Conf. on Intelligent Robots and Systems, 2008. IROS 2008*, pages 3622–3627, 2008.

[12] C. Ferrari and J. Canny. Planning optimal grasps. In *Robotics and Automation, 1992. Proceedings., 1992 IEEE Intl. Conf. on*, pages 2290–2295 vol.3, 1992.

[13] A. Hauck, J. Ruttinger, M. Sorg, and G. Farber. Visual determination of 3D grasping points on unknown objects with a binocular camera system. In *1999 IEEE/RSJ Intl. Conf. on Intelligent Robots and Systems, 1999. IROS '99. Proceedings*, volume 1, pages 272–278 vol.1, 1999.

[14] K. Huebner and D. Kragic. Selection of robot pre-grasps using box-based shape approximation. In *Intelligent Robots and Systems, 2008. IROS 2008. IEEE/RSJ Intl. Conf. on*, pages 1765—1770, 2008.

[15] M. T. Mason, A. Rodriguez, S. Srinivasa, and A. Vazquez. Autonomous manipulation with a general-purpose simple hand. *The Intl. Journal of Robotics Research*, 2011.

[16] M. T. Mason, S. Srinivasa, and A. S. Vazquez. Generality and simple hands. In *Robotics Research*, volume 70, pages 345–361. Springer, 2011.

[17] A.T. Miller and P.K. Allen. Graspit! a versatile simulator for robotic grasping. *Robotics & Automation Magazine, IEEE*, 11(4):110–122, 2004.

[18] A.T. Miller, S. Knoop, H.I. Christensen, and P.K. Allen. Automatic grasp planning using shape primitives. In *Robotics and Automation, 2003. Proceedings. ICRA '03. IEEE Intl. Conf. on*, volume 2, pages 1824–1829 vol.2, 2003.

[19] A. Morales, P. J. Sanz, A. P. del Pobil, and A. H. Fagg. Vision-based three-finger grasp synthesis constrained by hand geometry. *Robotics and Aut. Sys.*, 54(6):496–512, 2006.

[20] V. -D Nguyen. Constructing force-closure grasps. In *1986 IEEE Intl. Conf. on Robotics and Automation. Proceedings*, volume 3, pages 1368– 1373, 1986.

[21] V. -D Nguyen. Constructing stable grasps in 3D. In *1987 IEEE Intl. Conf. on Robotics and Automation. Proceedings*, volume 4, pages 234– 239, 1987.

[22] J. K. O'Regan and A. Noë. A sensorimotor account of vision and visual consciousness. *Behavioral and Brain Sciences*, 24(5):939–973, 2001.

[23] R. Platt, A. H Fagg, and R. A Grupen. Null-space grasp control: theory and experiments. *Robotics, IEEE Transactions on*, 26(2):282–295, 2010.

[24] M. Santello, M. Flanders, and J. F. Soechting. Postural hand synergies for tool use. *The Journal of Neuroscience*, 18(23):10105 –10115, 1998.

[25] A. Saxena, J. Driemeyer, and A. Y Ng. Robotic grasping of novel objects using vision. *The Intl. Journal of Robotics Research*, 27(2):157, 2008.